HHS Public Access

Author manuscript

Xenotransplantation. Author manuscript; available in PMC 2023 May 24.

Published in final edited form as:

Xenotransplantation. 2022 March ; 29(2): e12725. doi:10.1111/xen.12725.

Effects of human TFPI and CD47 expression and selectin and integrin inhibition during GalTKO.hCD46 pig lung perfusion with human blood

Shuhei Miura[1,2], **Zahra A. Habibabady**[1], **Franziska Pollok**[1,3], **Margaret Connolly**[1], **Shannon Pratts**[1], **Amy Dandro**[4], **Lori Sorrells**[4], **Kasinath Karavi**[4], **Carol Phelps**[4], **Will Eyestone**[4], **David Ayares**[4], **Lars Burdorf**[1], **Agnes Azimzadeh**[1,#], **Richard N. Pierson III**[1]

[1]Center for Transplantation Sciences, Department of Surgery, Massachusetts General Hospital, Boston, Massachusetts, USA

[2]Department of Cardiovascular Surgery, Teine Keijinkai Hospital, Sapporo, Japan

[3]Department of Anesthesiology, University Hospital Hamburg-Eppendorf, Hamburg, Germany

[4]RevivicorInc, Blacksburg, Virginia, USA

Abstract

Background: Loss of barrier function when GalTKO.hCD46 porcine lungs are perfused with human blood is associated with coagulation pathway dysregulation, innate immune system activation, and rapid sequestration of human formed blood elements. Here, we evaluate whether genetic expression of human tissue factor pathway inhibitor (hTFPI) and human CD47 (hCD47), alone or with combined selectin and integrin adhesion pathway inhibitors, delays GalTKO.hCD46 porcine lung injury or modulates neutrophil and platelet sequestration.

Methods: In a well-established paired *ex vivo* lung perfusion model, GalTKO.hCD46.hTFPI.hCD47 transgenic porcine lungs (hTFPI.hCD47, $n = 7$) were compared to GalTKO.hCD46 lungs (reference, $n = 5$). All lung donor pigs were treated with a thromboxane synthase inhibitor, anti-histamine, and anti-GPIb integrin-blocking Fab, and were pre-treated with Desmopressin. In both genotypes, one lung of each pair was additionally treated with PSGL-1 and GMI-1271 (P- and E-selectin) and IB4 (CD11b/18 integrin) adhesion inhibitors ($n = 6$ hTFPI.hCD47, $n = 3$ reference).

Correspondence: Shuhei Miura, Center for Transplantation Sciences and Division of Cardiac Surgery, Department of Surgery, Massachusetts General Hospital, 149 13th Street, MGH East, Room 9019, Charlestown, MA 02129-2020, USA. miura-sh@keijinkai.or.jp, smiura1024@outlook.jp.

AUTHOR CONTRIBUTIONS

Concept and design: Shuhei Miura, Agnes Azimzadeh, Richard N. Pierson III. Data collection: Shuhei Miura, Lars Burdorf, Zahra A. Habibabady, Franziska Pollok, Margaret Connolly, Shannon Pratts. Critical scientific contributions: Zahra A. Habibabady, Franziska Pollok, Margaret Connolly, Agnes Azimzadeh, Richard N. Pierson III. Providing of transgenic pigs: Amy Dandro, Lori Sorrells, Kasinath Karavi, Carol Phelps, Will Eyestone, David Ayares. Data analysis and interpretation: Shuhei Miura, Lars Burdorf, Agnes Azimzadeh, Richard N. Pierson III. Statistics: Shuhei Miura. Drafting article: Shuhei Miura. Critical revision: Shuhei Miura, Richard N. Pierson III. Approval of article: Shuhei Miura, Lars Burdorf, Richard N. Pierson III.

[#]Posthumous

SUPPORTING INFORMATION

Additional supporting information may be found in the online version of the article at the publisher's website.

Results: All except for two reference lungs did not fail within 480 min when experiments were electively terminated. Selectin and integrin adhesion inhibitors moderately attenuated initial pulmonary vascular resistance (PVR) elevation in hTFPI.hCD47 lungs. Neutrophil sequestration was significantly delayed during the early time points following reperfusion and terminal platelet activation was attenuated in association with lungs expressing hTFPI.hCD47, but additional adhesion pathway inhibitors did not show further effects with either lung genotype.

Conclusion: Expression of hTFPI.hCD47 on porcine lung may be useful as part of an integrated strategy to prevent neutrophil adhesion and platelet activation that are associated with xenograft injury. Additionally, targeting canonical selectin and integrin adhesion pathways reduced PVR elevation associated with hTFPI.hCD47 expression, but did not significantly attenuate neutrophil or platelet sequestration. We conclude that other adhesive mechanisms mediate the residual sequestration of human formed blood elements to pig endothelium that occurs even in the context of the multiple genetic modifications and drug treatments tested here.

Keywords

CD47; integrin; lung xenotransplantation; selectin; TFPI

1 | INTRODUCTION

Xenotransplantation is a promising future treatment option for patients with end-stage organ failure, potentially solving the limited availability of human donor organs.[1–3] The physiological and anatomical similarities between porcine and human, as well as the feasibility of modifying porcine genetics to address physiologic incompatibilities, make this species attractive as a potential organ source for clinical xenotransplantation.[4] Genetic modifications tested to date include removal of the primary carbohydrate target of preformed human anti-pig “natural” antibodies on porcine cells by α1,3-galactosyl transferase knockout (GalTKO), introduction of human complement regulatory proteins (hCRPs) such as hCD46, hCD55, and hCD59, and introduction of coagulation pathway regulatory gene additions such as hCD39, human thrombomodulin (hTBM) and human endothelial cell protein C receptor (hEPCR); several combinations of these genetic modifications are associated with prolonged xenograft survival in a various model.[5–9] For example, the use of GalTKO.hCD46.hTBM porcine donors has enabled survival of heterotopic hearts in baboons for over 2 years,[10] and recipients of life-supporting GalTKO.hCD46 kidneys have survived for greater than 6 months.[11] On the other hand, survival of baboons that received a porcine lung transplant has generally been limited to a few days and a maximum of 31 days.[12–14]

GalTKO.hCD46 porcine lungs perfused *ex vivo* with human blood rapidly sequester the majority of circulating platelets and neutrophils, and the majority of lungs fail within the 8 h in association with prolific activation of coagulation and inflammation. A candidate intervention to prevent coagulation dysregulation is expression of human tissue factor pathway inhibitor (hTFPI), which is a direct inhibitor of activated extrinsic coagulation pathway factors such as Va, VIIa, and Xa. Specifically, incompatibility between porcine TFPI and human coagulation pathway molecules, including tissue factor, may contribute to failure of thromboregulation after lung xenotransplantation,[15] although other investigators have presented evidence contradicting this assertion.[16] Similarly, CD47 is a self-recognition

protein that inhibits phagocytosis of cells expressing CD47 by ligating signal-regulatory protein alpha (SIRPa) and triggering a negative regulatory ‘‘don’t eat me” signal to SIRPa-expressing cells, such as macrophages. Transgenic expression of hCD47 on porcine cells prevents cross-species inflammatory dysregulation by overcoming the known species incompatibility between porcine CD47 and primate SIRP-α, and is thus expected to inhibit innate immune system activation and associated inflammation.[17–19] Supporting this hypothesis, Yamada et al.[20] have presented evidence that GalTKO porcine lungs expressing hCD47 on both endothelium and alveolar epithelium improved lung recipient survival in an in vivo pig-to-baboon xeno lung transplantation model.

As part of our ongoing studies to understand and prevent the early failure of lung xenografts, here we asked whether co-expression of hTFPI and hCD47 on the GalTKO.hCD46 background might confer protection from the coagulation and inflammatory dysregulation phenomena associated with lung xenograft injury. Taking advantage of our paired lung xenograft model, we additionally asked whether selectin- and integrin-mediated leukocyte and platelet sequestration contribute significantly to residual endothelial damage and coagulation cascade amplification in the context of hTFPI and hCD47 expression. Selectins are a family of cellular adhesion molecules that canonically mediate platelet and leukocyte adhesion under flow conditions in the setting of inflammation associated with ischemia reperfusion injury and allograft rejection. Integrins are transmembrane receptors for extracellular ligands that function alongside selectins to mediate cell adhesion and translocation, in addition to facilitating cell adhesion to the extracellular matrix.[21,22] We hypothesized that simultaneously interfering in selectin and integrin-mediated cell adhesion pathways using cell adhesion inhibitors such as PSGL-1 (targeting P- and E-selectin)[23] and GMI-1271 (a carbohydrate mimic specific for E-selectin)[24] as well as IB4 (a CD11b/CD18 integrin-blocking Fab)[25] and 6B4 (a GP1b integrin-blocking Fab) might reduce platelet adhesion and neutrophil rolling, further modulate coagulation dysregulation and innate inflammatory cell activation, and contribute to prolong GalTKO.hCD46.hTFPI.hCD47 lung xenograft survival during *ex vivo* perfusion with human blood.

2 | MATERIALS AND METHODS

2.1 | Animals

Genetically engineered GalTKO.hCD46 pigs (n = 12, BW 15–80 kg) were supplied by Revivicor (Blacksburg, VA), 7 of which additionally expressed hTFPI and hCD47 (GalTKO.hCD46.hTFPI.hCD47: hTFPI.hCD47). Human CD46 expression was homozygous in all donor pigs studied here. All procedures were approved by the Institutional Animal Care and Use Committee at Massachusetts General Hospital and were conducted in compliance with National Institutes of Health guidelines for the care and use of laboratory animals.

2.2 | Lung harvest

The donor pigs received DDAVP pre-treatment (Desmopressin Acetate, Diamondback Drugs, Scottsdale, AZ; 3 μg/kg BW) IV prior to organ procurement) to reduce pulmonary vascular vWF expression.[26] Induction of anesthesia and surgical organ dissection were

performed as previously described.[27] Prior to donor exsanguination and flushing the lungs antegrade with Perfudex lung preservation solution, 1-benzylimidazole (1-BIA, 5 mg/kg BW; Sigma–Aldrich), and synthetic prostaglandin I_2 (0.06 mg/kg, Remodulin (reprostinil), United Therapeutics) were administered intravenously and allowed to circulate for several minutes.

2.3 | Lung perfusion

The right and left lungs were separately perfused via the pulmonary artery (PA) using side-by-side circuits fashioned from silicon tubing and polyurethane connectors as previously described.[28] PA flow was measured and recorded with a flowmeter (Transonic Systems Inc., Model TTFM 73–0146). The Digimed System Integrator (Micro-Med) continuously recorded PA and airway pressures (AWP) via transducers integrated into the perfusion (Ismatec MCP rollerpump, IDEX) and ventilator (Harvard apparatus respirator, model 613) circuits, respectively, using PowerLab 16/35 and LabChart 7 pro (AD Instruments). Lungs were ventilated at 15 breath/min (tidal volume approximately 10 ml/kg). Pulmonary vascular resistance (PVR) was estimated using the equation: PVR = pulmonary artery pressure/ pulmonary artery flow. Lung survival time was defined as the interval after initiation of lung perfusion when the lung function reached one of three ‘lung failure’ criteria: (a) PVR > 600 mm Hg*min/L; (b) development of gross tracheal edema filling the endotracheal tube; or (c) intraparenchymal sequestration of > 85% of the reservoir’s perfusate volume. If lungs did not meet a “survival” criterion, experiments were electively terminated after 480 min of perfusion.

2.4 | Perfusate preparation

Fresh whole blood was collected from two healthy human blood donors (~450 ml each) into a blood collection bag containing 64 ml of CPDA-1. Two units (~240 ml each) of type-compatible thawed plasma were added for each unit of blood to obtain an initial perfusate volume of ~2 L with a pre-perfusion hematocrit of ~16%. Heparin (3 IU/ml blood, Heparin Sodium Injection, Sagent), calcium chloride (1.3–1.6 mg/ml blood, American Regent, Inc.) to neutralize the CPDA chelating agent, and 8.4% sodium bicarbonate (up to 0.8 mg/ml blood, target pH of 7.36–7.44, Hospira, Inc.) were added to the blood pool. All blood components were thoroughly mixed before circuit priming. The blood was uniformly treated with a thromboxane synthase inhibitor (1-BIA, 112 mg/L), anti-histamine (Famotidine, 11.2 mg/L) and anti-GPIb integrin-blocking Fab (6B4, an Fab that blocks the human GPIb binding site for human or porcine vWF, 10 mg/L) based on our prior observations in this model.[28]

2.5 | Experimental groups

In *ex vivo* lung perfusion model, hTFPI.hCD47 transgenic lungs ($n = 7$) were perfused with fresh heparinized human blood and compared to GalTKO.hCD46 lungs (reference; $n = 5$). In the majority of paired circuits of both genotypes, one lung of each pair ($n = 6$ for hTFPI.hCD47; $n = 3$ for GalTKO.hCD46) was additionally treated with selectin (PSGL-1, 19.1 mg/ml; GMI, 50 mg/ml) and integrin (IB4, 5.5 mg/ml) adhesion inhibitors. Three lungs were excluded from the analysis: one hTFPI.hCD47 expressing lung because of a technical

problem; and two GalTKO.hCD46 lungs because a different combination of drugs were used in the contralateral lung.

2.6 | Sampling regimen

Baseline blood samples were taken after blood preparation ("pre" sample), and after drug addition and circulating the blood in the perfusion circuit for at least 5 min (time 0 sample). Further samples were collected from the pulmonary veins at 5, 15, 30, 60, 120, 240, 300, 360, 420 and 480 min after lung perfusion was initiated. After centrifugation, plasma samples were stored at −80°C until analysis. Lung tissue samples were collected pre-perfusion and 10, 30, 60, 120, 240, 300, 360 and 480 min of perfusion.

2.7 | Hematologic analysis

Formed blood cell counts were enumerated by standard automated techniques (Antech Diagnostics and Hemavet 950FS Hematology Analyzer, Drew Scientific in duplicate) in samples collected into ethylenediaminetetraacetic acid (EDTA).

2.8 | Flow cytometry

Blood samples were stained by monoclonal antibodies specific for CD41 (as marker for platelets) (AbD Serotec) and CD62P (expressed by activated platelets) (BD Pharmingen) and acquired on a FACSCalibur (BD Biosciences). Platelets and platelet aggregates, identified by size and presence of CD41 staining, were analyzed for expression of CD62P by FACS analysis. Results were expressed as percentage of CD62P-positive cells among CD41-positive cells.

2.9 | F1+2 and Beta-thromboglobulin enzyme-linked immunosorbent assays

Beta-thromboglobulin (βTG) and prothrombin fragments 1+2 (F1 + 2), as a measure of platelet (βTG) and coagulation cascade activation (F1+2), were assayed by commercially available enzyme-linked immunosorbent assay (ELISA) kits (Asserachrom βTG, Diagnostica Stago S.A.S, Asnières sur Seine Cedex France; Enzyngost® F1+2 monoclonal (assay), Siemens Healthcare Diagnostics Products GmbH, Marburg, Germany) using plasma samples collected in CTAD tubes. Quantitative concentrations of βTG (in IU/ml) and F1+2 (in nmol/L), respectively, were measured by the difference in optical density detected at 450 nm wavelength using a spectrophotometer (SpectraMax® iD3) in reference to a standard curve.

2.10 | Wet-to-dry weight ratio

Tissue edema at the time of elective termination was approximated by sampling a portion of the upper lower lung lobe; samples from two lungs failing before this time point were excluded from this analysis. Tissue weight was measured immediately after collection, as well as after completely drying under a chemical fume hood over ~2 weeks. Data are represented as wet-to-dry weight ratio (WDR).

2.11 | Histology and immunochemistry

Lung biopsies obtained during the perfusion and terminally samples were trisected, processed as previously described[29] and compared to pre-perfusion sample.

Formalin fixed, paraffin-embedded sections were stained with hematoxylin and eosin (H&E) for light microscopy and analyzed qualitatively for the presence of intravascular thrombosis, and interstitial, alveolar or larger airway edema and hemorrhage.

Expression of hTFPI and hCD47 on porcine lung was assessed by immunohistochemistry (IHC). Pre-lung tissue samples of donor porcine were collected and staining performed on formalin-fixed, paraffin-embedded tissues. Samples were sectioned at 3 μm, allowed to air-dry, deparaffinized in xylene and rehydrated through graded alcohols to water. Antigen retrieval was performed using the Biocare decloaking chamber for 15 min at 110°C in Diva retrieval solution (Biocare: DV2004LX). Endogenous peroxidases were quenched using Dual Endogenous Enzyme Block (DEEB; Agilent Technologies S2003) for 10 min. After washing with TBS-Tween buffer (Sigma cat: T9039), sections were blocked with Serum Free Protein Block (Agilent Technologies: X0909) for 5 min. Sections were stained with 100 μl of anti-human hTFPI (Santa Cruz #SC-133139, dilution 1:100) and anti-human CD47 (BD Biosciences #556044, dilution 1:500) antibodies and allowed to incubate at room temperature for 30 min. After incubation, slides were rinsed in wash buffer and then incubated in 100 μl of EnVision+ Dual HRP secondary with 0.5% pig serum (Agilent K406189–2) for 30 min. Antibody binding was then detected using a five-minute incubation of 100 μl of diaminobenzidine tetrahydrochloride (DAB; Agilent Technologies: K346811–2). Slides were rinsed in running tap water, counterstained with hematoxylin (VWR: 3801575) dehydrated through graded alcohols and xylene, mounted with glass coverslips and imaged.

2.12 | Statistical analysis

All data are presented as mean and standard deviation (SD) for all variables except for cumulative lung survival time, which is expressed as median. Continuous variables were checked for normality. Variables that were normally distributed were assessed with a one-way analysis of variance (ANOVA) test or the Student *t*-test. Those that were not normally distributed were analyzed using the Mann–Whitney non-parametric test. *P*-values < 0.05 were considered statistically significant. All statistical analyses were performed with GraphPad Prism (Version 9.1.2).

3 | RESULTS

3.1 | hTFPI and hCD47 expression vector

Design and targeting strategy of the hTFPI and hCD47 expression vector. The hTFPI–hCD4 membrane anchor[30] and hCD47 transgenes were driven by a ubiquitously expressing CAG promoter to generate a single peptide subject to cleavage at the T2A sequence. The vector was targeted to a previously inserted NeoR sequence in exon 9 of porcine GGTA1,[31] using homology-directed repair facilitated by Crispr/Cas9 (Figure S1). To generate transgenic pigs, vector fragments were transfected into primary porcine fetal fibroblasts. Correctly

targeted, single-cell clones bearing single copy, monoallelic (hemizygous) insertions of the vector were used for somatic cell nuclear transfer (SCNT[32];). SCNT embryos were transferred to recipient females to generate pigs. Expression of hTFPI and hCD47 in pig tissues was confirmed by IHC and western blot (data not shown).

3.2 | Graft survival time of *ex vivo* perfused lungs

All but two reference lungs did not fail within 480 min when experiments were electively terminated (Figure 1); one reference lung showed an increase in PVR over 600 mmHg at 183 min and the other lung failed due to trachea edema at 440 min. All hTFPI.hCD47 lungs, with or without additional selectin and Integrin adhesion inhibitor, survived to the elective termination; their survival was not significantly increased when compared to reference lungs ($P = 0.068$).

3.3 | Pulmonary function parameters

With one exception (one reference lung, noted above), all lungs with both genotypes maintained low-range and very stable PVR values throughout the perfusion (Figure 2). hTFPI.hCD47 lungs treated with additional selectin and integrin adhesion inhibitors tended toward lower PVR during the first 2 h of perfusion (e.g., $P = 0.074$ at 60 min and $P = 0.081$ at 90 min), but this trend did not achieve conventional statistical significance. Similarly, the trend toward lower AWP in association with hTFPI.hCD47 lungs treated with additional adhesion inhibitor did not achieve significance (Figure S2).

3.4 | Neutrophil and monocyte enumeration during lung perfusion

Neutrophil (PMN) sequestration from the perfusate was observed after initiation of lung perfusion in all experimental groups (Figure 3). During the first hour of perfusion, PMN sequestration was significantly delayed in association with hTFPI.hCD47 expression (84 ± 36 for hTFPI.hCD47; vs. 36% ± 27% for reference at 30 min [$P < 0.05$]; 58 ± 28 vs. 22% ± 20% at 60 min [$P < 0.05$]). At elective termination at 480 min, only 8 (± 3)% of the initial PMN count remained circulating in reference experiments, whereas in hTFPI.hCD47 experiments 29 (± 35)% of neutrophils were still present in the perfusate ($p < 0.0001$). Treatment with selectin and integrin adhesion inhibitors did not significantly modulate PMN sequestration in association with either lung phenotype.

Monocyte counts increased 1.5–3.5 fold during the first 45 min of *ex vivo* perfusion. The largest proportional (to 350% of baseline, Figure 4A) and absolute (to 519 ± 21 monocytes/ul, Figure 4B) increases in circulating monocytes were observed at 5 min in association with the reference GalTKO.hCD46 lung phenotype, although the quantitative difference between reference and hTFPI.hCD47 groups did not reach statistical significance (e.g., the absolute monocyte counts were 269 ± 23/ul for hTFPI.hCD47 vs. 519 ± 21/ul for GalTKO.hCD46 at 5 min: $P = 0.069$). Subsequent declines in monocyte counts were not significantly inhibited in association with hTFPI.hCD47 expression. Selectin and Integrin adhesion inhibitor treatment did not significantly modulate monocyte counts over the course of lung perfusion in association with either lung phenotype.

3.5 | Platelet sequestration and activation

In all groups, platelet sequestration of 40%–80% was detected by the initial measurement at 5 min after start of perfusion. Platelet sequestration was not significantly delayed in association with hTFPI.hCD47 expression, with or without selectin and integrin adhesion inhibitors. All groups exhibited similar downward trends through perfusion; for example, only 8 (± 4) % of the initial platelets were still detectable in the hTFPI.hCD47 group perfusate at 480 min (Figure 5A). Activation of residual circulating platelets, as CD62P expression, showed a similar trend during first 2 h of perfusion in all lungs. However, hTFPI.hCD47-expressing lungs were associated with circulating platelet activation toward the end of perfusion that was significantly decreased compared to that in reference GalTKO.hCD46 lung perfusate (Δ%CD62P positive at 480 min: 1.0±3.0 for hTFPI.hCD47 vs. 18.0%±10.0% for reference, [$p < 0.0001$]) (Figure 5B). hTFPI.hCD47-expressing lungs were also associated with significantly lower overall platelet activation as measured by β-thromboglobulin (βTG) levels (308±103 for hTFPI.hCD47) than in reference lung (1154±444 IU/ml for GalTKO.hCD46, [$p = 0.036$]) at 480 min (Figure 5C).

3.6 | Coagulation cascade activation for hTFPI function

Delta F1+2 values showed a similar trend during first 2 h of perfusion independent of genotype or selectin/integrin blockade (Figure 6). Thereafter, the trend toward reduced coagulation cascade activation associated with hTFPI.hCD47-expressing lungs reached statistical significance compared to that in reference GalTKO.hCD46 lungs by the end of perfusion (e.g., 4.0±2.0 for hTFPI.hCD47 vs. 33.7±28.3 nmol/L for reference at 480 min; [$p = 0.0393$]) (Figure 6).

3.7 | Wet-to-dry weight ratio

Treatment with selectin/integrin inhibitors (5.0 ± 0.1) or hTFPI.hCD47 expression (4.0 ± 1.0) was associated with significantly lower terminal WDR compared to reference lungs (7.0 ± 1.0; $p = 0.0517$ vs. selectin/integrin inhibition, $p = 0.0073$ vs. hTFPI.hCD47), reflecting reduced sequestration of perfusate volume in the lung (Figure 7). WDR after treatment with additional adhesion inhibitors in hTFPI.hCD47 lungs (4.8 ± 0.2) did not differ compared to hTFPI.hCD47 alone, but WDR increase remained significantly attenuated compared to reference lungs (4.8 ± 0.2 vs. 7.0 ± 1.0, $p = 0.0358$).

3.8 | Histology and immunochemistry

Tissue samples collected before initiation of xenogenic perfusion (“pre” sample) displayed almost normal microscopic lung anatomy with air-filled alveoli and thin inter-alveolar septae, although with diffuse mild interstitial inflammation (Figure 8). Biopsies taken at the time of elective termination (“final” sample), samples collected from GalTKO.hCD46 lung revealed severe interstitial inflammation with bronchial epithelial inflammation. However, lungs expressing hTFPI.hCD47 showed relatively well-conserved lung tissue with only mild congestion and interstitial inflammation.

Expression of hTFPI and hCD47 on donor porcine lungs was confirmed by IHC using anti-human TFPI and CD47 antibodies (Figure 9). Positive staining was demonstrated by a deposition of brown pigment at the site of antibody binding. hTFPI was strongly and

prevalently expressed in alveolar septal locations consistent with endothelium in addition to prominent expression within airway epithelial cells and tissue and airway leukocytes (Figure 9C). hCD47 was expressed mainly on alveolar epithelium and on leukocytes; faint linear hCD47 staining was detected in about 30% of interalveolar septae in a pattern consistent with endothelial expression (Figure 9D). No significant variation was observed in the pattern of hCD47 or hTFPI protein expression between the 3 hTFPI.hCD47 lungs examined by IHC.

4 | DISCUSSION

Lung xenograft rejection is associated with activation of numerous inflammatory and coagulation pathways.[27] Here, we show that in the *ex vivo* lung model, expression of hCD47 with hTFPI confers modest protective effects for GalTKO.hCD46 transgenic organs. This observation supports our working hypothesis that recipient leukocytes, including monocyte/macrophage lineage cells, are activated at least in part due to the absence of self-recognition molecules, including hCD47, resulting in activation of blood leukocytes mediated by the CD47-SIRPα pathway. CD47 expression on the endothelium was relatively low, raising the possibility that approaches to increase CD47 expression may be associated with improved protection, as previously reported by Yamada.[20] In addition, expression of additional self-recognition molecules such as HLA-E may provide synergistic effects through additional inhibition of NK cell activation, as suggested by our prior work.[33] Incomplete efficacy of these modifications could also be explained by leukocyte, monocyte, and platelet expression of Fc receptors, selectins, and integrins, including multiple receptors responsive to fibrin and coagulation cascade by products. Ligation of each of these receptor families generally promotes activation of formed blood elements, as do the panoply of proinflammatory cytokines elaborated by multiple cell populations in both donor and recipient origin.

hTFPI was included in the GalTKO.hCD46.hTFPI.hCD47 pig gene construct in part to address the thrombodysregulation that we and others have observed in association with cell and organ xenograft injury and failure. Statistically significant if biologically modest effects were observed in association with hTFPI expression, including attenuated late βTG elaboration, decreased F1+2 thrombin formation, reduced neutrophil sequestration and platelet activation, and attenuation of lung fluid accumulation. We consider this as indirect evidence that the hTFPI modification, intended to mute TF-associated clot propagation, endothelial activation, and loss of vascular barrier function, may partially address one of these several known thrombodysregulatory mechanisms that have been identified to date.

This work was undertaken in the context of our prior work describing endothelial dysfunction and loss of vascular barrier function despite several other fundamentally important porcine genetic modifications. Introduction of GalTKO porcine eliminates the immune response mediated by anti-Gal antibody,[34,35] but does not eliminate important effects associated with other anti-carbohydrate antibodies or preformed human antibodies that might cross-react with other pig antigens. The addition of hCRPs (hCD46, hCD55, hCD59) reduces the complement driven organ injury.[36–38] When these genetic modifications are combined, GalTKO.hCD46 porcine lungs exhibit early graft failure associated with inflammatory and coagulation dysregulation. This observation justifies efforts to explore:

(1) removing the two other dominant carbohydrate targets (Neu5Gc; β4 Gal)[39]; (2) adding coagulation pathway regulatory genes such as hCD39,[40] hTBM,[41] and hEPCR,[42] and increasing intensity and prevalence of endothelial expression of hTFPI[15] to improve coagulation cascade dysregulation; and (3) expressing self-recognition receptors such as HLA-E[33] and increasing intensity and/or prevalence of endothelial expression of hCD47[17–19] to blunt innate immune inflammation.

In vitro, expression of hCD47 on porcine cells not only suppressed the activation of human macrophages but also production of proinflammatory cytokines including TNF-α, IL-1β, and IL-6, and inhibits macrophage-mediated porcine cell cytotoxicity.[43] In vivo, porcine lungs expressing hCD47 both on alveolar epithelium and endothelium remained viable by histology for over 7 days in a pig-to-baboon lung transplant model.[20] Although these results suggest that hCD47-expressing GalTKO porcine lungs may offer some protection for organ xenografts, CD47 effect alone appears not to be sufficient to prevent macrophage-mediated endothelial damage. Recent studies have demonstrated that thrombospondin-1 (TSP-1), another CD47 ligand, prevents CD47 from binding to SIRP-α, thus inhibiting suppression of the phagocyte function. However, because hTFPI also binds to TSP-1, it may reduce competition by TSP-1 for CD47 binding to SIRP-α.[44,45] That is, on balance co-expression of hCD47 and hTFPI is expected to not only reduce thrombosis mediated by porcine tissue factor but also enhance suppression of macrophage phagocytosis mediated by hCD47-SIRP-α signaling.[46] Our results demonstrate that the expression of hTFPI and hCD47 on porcine lungs inhibited decline in lung vascular barrier function, reflected by lower tissue edema (WDR), delayed PMN sequestration, and attenuated platelet activation. However, our experiments do not enable elucidation of the relative contributions of each pathway to the effects observed.

In addition to genetic modifications, pharmacological interventions could potentially abort the cascade of events that contribute to endothelial damage, and thus potentially to early lung failure, by preventing the initial sequestration of leukocytes. Laird et al.[47] have showed that when resting porcine aortic endothelial cells (PAECs) are exposed to whole human blood under physiologic flow conditions, porcine endothelium activated in response to inflammatory human cytokines exhibit significantly increased P- and E-selectin expression. In that model, both P- and E- selectin antagonism significantly decreased neutrophil rolling, and neutrophil adhesion, and endothelial damage in a dose-dependent manner. The efficacy of PSGL-1 (a natural ligand for P-selectin)[23] and GMI-1271 (an E-selectin antagonist developed by GlycoMimetics, Inc.)[24] and other molecules have previously been shown to prevent neutrophil migration, reduce monocyte recruitment, accelerate thrombolysis, inhibit platelet binding to injured vascular endothelium, and reduce ischemia-reperfusion injury in myocardial, renal, intestine and hepatic models.[48–53] However, in other lung models, previous studies in other non-xeno settings such as acute respiratory distress syndrome showed that selectin inhibition alone was not effective, but when combined with integrin inhibition neutrophil sequestration was reduced.[54–56] Based on these reports, we hypothesized that interfering in selectin and integrin-mediated cell interaction pathways together might predict to reduce neutrophil and platelet sequestration, and attenuate associated endothelial damage in the physiologic *ex vivo* lung xeno perfusion model. Our study showed that additional adhesion inhibition using selectin and integrin blockade

transiently reduced PVR elevation associated with hTFPI.hCD47 expression and inhibited WDR increase for reference lungs, but it did not significantly attenuate neutrophil or platelet sequestration by either lung genotype. However, this pharmacologic adhesion inhibition was associated with relatively preserved lung physiology, function, and morphology despite evidence that inflammation and coagulation pathway dysregulation mechanisms are not completely inhibited.

Multiple recipient-directed pharmacologic interventions—integrin-blocking αGPIb Fab, thromboxane synthase inhibitor, and anti-histamine—were used consistently in these studies to protect a pig lung xenograft from previously identified mechanisms of injury based on our prior experiments[28,57] and those of others.[26] Porcine von Willebrand factor (vWF) binds to GPIb on human platelets in the absence of shear stress, resulting in platelet activation and aggregation.[58] Similar protective effects previously reported for platelet activation using αGPIb in reference GalTKO.hCD46 lungs were observed in the GalTKO.hCD46.hTFPI.hCD47 lungs studied here (Figure S3).

Administration of desmopressin (DDAVP) to donor porcine prior to lung harvest depletes endothelial porcine vWF[26,58] and in combination with recipient aGPIb antagonist treatment[28] was shown to attenuate platelet activation by blocking non-physiologic ligation to quiescent porcine vWF. However, the use of DDAVP would be expected to increase endothelial P- (and E-)selectin expression, and to promote leukocyte rolling in post-capillary venules, thus theoretically amplifying platelet adhesion by that alternative mechanism.[47,59] Our approach in the current study addressed this issue, predicting that use of a P-selectin inhibitor might attenuate this potentially undesirable side effect of DDAVP administration. At least until alternative methods to overcome porcine vWF-mediated coagulation dysfunction are developed, such as “humanizing” the GPIb binding sites on porcine vWF,[60] we advocate to combine DDAVP with P-selectin inhibition in our future work.[61] Similarly, until the upstream triggers for elaboration of inflammatory molecules are better understood and dependably controlled, our lung work will continue to deploy demonstrably effective lung protective pharmacologic interventions. These currently include thromboxane synthase inhibition (1-benzylimidazole[62,63]), histamine receptor blockade (diphenhydramine, famotidine[64,65]) and selectin inhibition, each of which has been shown to significantly improve one or more parameters of lung function in our *ex vivo* model.[66]

This study’s statistical power was limited by the relatively small number of experiments, particularly for those in which reference GalTKO.hCD46 lungs were treated with selectin and integrin inhibitors. In addition, because of the complexity and cost of creating genetically modified pigs and the infeasibility of discerning pathway-specific down-stream molecular effects for each pathway, we are unable to independently evaluate the functional contributions of hCD47 or hTFPI. Similarly, given the limited number of lungs available for the study, we were unable to separately evaluate the effects of selectin versus integrin blockade in this lung perfusion model. However, most importantly, we clearly demonstrate that the combination of gene modifications and drug treatment studied here was insufficient to prevent platelet and leukocyte sequestration and activation. This observation constructively focuses our future work on other additional pathways and justifies additional genetic engineering and alternative pharmacologic approaches outlined above to better

understand lung xenograft injury and ultimately to learn how to prevent it. We observed higher PVRs in association with hTFPI.hCD47 compared to reference lungs. Since the lead experimentalist for this work (LB) was consistent throughout this series, we consider it unlikely that a systematic change in conduct of the experiments occurred. Maximum PA flow is set by protocol based on pig weight, which varies by pig age when the lungs are studied. Growth characteristics differ between various pig genotypes, and pulmonary vasoreactivity may change at different rates than does pig weight. Although pigs were generally of similar age and weight ranges across the study groups reported here, we speculate that differences in pig physiologic maturity between pig genotypes at the age of the study is the most likely explanation for this unexpected finding.

The predictive value of the *ex vivo* perfusion model for the hTFPI.CD47 pig genotype, and others, has recently been tested in vivo[67]; good initial life-supporting function but early failure due to inflammation in the hTFPI.CD47 lung and in the recipient suggest that the proinflammatory and adhesive interactions seen *ex vivo* are associated with adverse consequences in vivo. We conclude that the *ex vivo* model remains mechanistically valuable even if protection from lung failure beyond 8 h is regularly observed.

In summary, expression of hTFPI.hCD47 on porcine lung is partially effective to attenuate inflammation and dysregulated coagulation, and thus may prove useful as part of an integrated strategy to prevent injury of lung xenografts, as previously reported for the liver.[68] However, we concluded that hTFPI and hCD47, at least as expressed in the animals studied here, and even when combined with pharmacologic treatment using selectin and integrin inhibitors, only transiently delayed, and did not completely prevent, neutrophil and platelet sequestration, and were not sufficient to prevent physiologically important lung xenograft injury in our *ex vivo* perfusion model.

Supplementary Material

Refer to Web version on PubMed Central for supplementary material.

ACKNOWLEDGMENTS

Funding for this study was supported by U19 AI090959, sponsored research agreements with Revivicor, Inc, and Lung Bioengineering PBC, and gifts from United Therapeutics. FP received funding from the German Heart Foundation (Deutsche Herzstiftung e.V.). This work was supported by the Center for Transplantation Sciences at Massachusetts General Hospital. Special thanks to Ivy A. Rosales, MD, Immunopathology Research Laboratory at Massachusetts General Hospital, for helping with the findings of lung histology.

Funding information

Revivicor, Inc, Grant/Award Number: U19 AI090959; German Heart Foundation (Deutsche Herzstiftung)

Abbreviations:

1-BIA	1-benzylimidazole, Thromboxane synthase inhibitor
AWP	Airway pressure
CPDA-1	citrate phosphate dextrose adenine solution

CTAD	Citrate, theophylline, adenosine, dipyridamole
DDAVP	Desmopressin
EDTA	ethylenediaminetetraacetic acid
ELISA	Enzyme-linked immunosorbent assay
F1+2	Prothrombin fragments 1+2
GalTKO	α1,3-galactosyl transferase knockout
H&E	hematoxylin and eosin
hCD39	human ectonucleoside triphosphate diphosphohydrolase 1, ENTPD1
hCD46	Human membrane cofactor protein, hMCP
hCD55	Human decay-accelerating factor, hDAF
hCD59	human MAC-inhibitory protein
hCRP	human complement regulatory protein
hEPCR	Human endothelial cell protein C receptor
hTBM	Human thrombomodulin, hCD141
hTFPI	human tissue factor pathway inhibitor
MONO	Monocyte
PA	Pulmonary artery
PAEC	Porcine aortic endothelial cell
PMN	polymorphonuclear leukocyte
PVR	Pulmonary vascular resistance
SIRPa	signal-regulatory protein alpha
vWF	von Willebrand factor
WDR	Wet-to-dry weight ratio
βTG	β-thromboglobulin

REFERENCES

1. Lamm V, Hara H, Mammen A, Dhaliwal D, Cooper DK. Corneal blindness and xenotransplantation. Xenotransplantation 2014;21(2):99–114. [PubMed: 25268248]
2. Kim MK, Choi HJ, Kwon I, et al. International Xenotransplantation Association. The International Xenotransplantation Association consensus statement on conditions for undertaking clinical trials of xenocorneal transplantation. Xenotransplantation 2014;21(5):420–430. [PubMed: 25176471]

3. Cooper DK, Satyananda V, Ekser B, et al. Progress in pig-to-non-human primate transplantation models (1998–2013): a comprehensive review of the literature. Xenotransplantation 2014;21(5):397–419. [PubMed: 25176336]
4. Sachs DH. The pig as a potential xenograft donor. Vet Immunol Immunopathol 1994;43(1–3):185–191. [PubMed: 7856051]
5. Cowan PJ, Cooper DK, d'Apice AJ. Kidney xenotransplantation. Kidney Int 2014;85(2):265–275. [PubMed: 24088952]
6. Byrne GW, McGregor CG. Cardiac xenotransplantation: progress and challenges. Curr Opin Organ Transplant 2012;17(2):148–154. [PubMed: 22327911]
7. Kim K, Schuetz C, Elias N, et al. Up to 9-day survival and control of thrombocytopenia following alpha1,3-galactosyl transferase knockout swine liver xenotransplantation in baboons. Xenotransplantation 2012;19(4):256–264. [PubMed: 22909139]
8. Yeh H, Machaidze Z, Wamala I, et al. Increased transfusion-free survival following auxiliary pig liver xenotransplantation. Xenotransplantation 2014;21(5):454–464. [PubMed: 25130043]
9. Hering BJ, Walawalkar N. Pig-to-nonhuman primate islet xenotransplantation. Transpl Immunol 2009;21(2):81–86. [PubMed: 19427901]
10. Mohiuddin MM, Singh AK, Corcoran PC, et al. Chimeric 2C10R4 anti-CD40 antibody therapy is critical for long-term survival of GTKO.hCD46.hTBM pig-to-primate cardiac xenograft. Nat Commun 2016;7:11138. [PubMed: 27045379]
11. Iwase H, Hara H, Ezzelarab M, et al. Immunological and physiological observations in baboons with life-supporting genetically engineered pig kidney grafts. Xenotransplantation 2017;24(2):10.1111.
12. Kubicki N, Laird C, Burdorf L, Pierson RN 3rd, Azimzadeh AM. Current status of pig lung xenotransplantation. Int J Surg 2015;23(Pt B):247–254. [PubMed: 26278663]
13. Cantu E, Gaca JG, Palestrant D, et al. Depletion of pulmonary intravascular macrophages prevents hyperacute pulmonary xenograft dysfunction. Transplantation 2006;81(8):1157–1164. [PubMed: 16641602]
14. Burdorf L, Laird CT, Harris DG, et al. Pig-to-baboon lung xenotransplantation: extended survival with targeted genetic modifications and pharmacologic treatments. Am J Transplant 2021;22(1):28–45. [PubMed: 34424601]
15. Chen D, Riesbeck K, McVey JH, et al. Regulated inhibition of coagulation by porcine endothelial cells expressing P-selectin-tagged hirudin and tissue factor pathway inhibitor fusion proteins. Transplantation 1999;68(6):832–839. [PubMed: 10515384]
16. Lee KF, Salvaris EJ, Roussel JC, Robson SC, d'Apice AJ, Cowan PJ. Recombinant pig TFPI efficiently regulates human tissue factor pathways. Xenotransplantation 2008;15(3):191–197. [PubMed: 18611227]
17. Okazawa H, Motegi S, Ohyama N, et al. Negative regulation of phagocytosis in macrophages by the CD47-SHPS-1 system. J Immunol 2005;174(4):2004–2011. [PubMed: 15699129]
18. Ide K, Wang H, Tahara H, et al. Role for CD47-SIRPalpha signaling in xenograft rejection by macrophages. Proc Natl Acad Sci U S A 2007;104(12):5062–5066. [PubMed: 17360380]
19. Navarro-Alvarez N, Yang YG. CD47: a new player in phagocytosis and xenograft rejection. Cell Mol Immunol 2011;8(4):285–288. [PubMed: 21258362]
20. Watanabe H, Sahara H, Nomura S, et al. GalT-KO pig lungs are highly susceptible to acute vascular rejection in baboons, which may be mitigated by transgenic expression of hCD47 on porcine blood vessels. Xenotransplantation 2018;25(5):e12391. [PubMed: 29527745]
21. Zarbock A, Ley K, McEver RP, Hidalgo A. Leukocyte ligands for endothelial selectins: specialized glycoconjugates that mediate rolling and signaling under flow. Blood 2011;118(26):6743–6751. [PubMed: 22021370]
22. Feng C, Zhang L, Almulki L, et al. Endogenous PMN sialidase activity exposes activation epitope on CD11b/CD18 which enhances its binding interaction with ICAM-1. J Leukoc Biol 2011;90(2):313–321. [PubMed: 21551251]
23. Abadier M, Ley K. P-selectin glycoprotein ligand-1 in T cells. Curr Opin Hematol 2017;24(3):265–273. [PubMed: 28178038]

24. Culmer DL, Dunbar ML, Hawley AE, et al. E-selectin inhibition with GMI-1271 decreases venous thrombosis without profoundly affecting tail vein bleeding in a mouse model. Thromb Haemost 2017;117(6):1171–1181. [PubMed: 28300869]
25. Graham IL, Gresham HD, Brown EJ. An immobile subset of plasma membrane CD11b/CD18 (Mac-1) is involved in phagocytosis of targets recognized by multiple receptors. J Immunol 1989;142(7):2352–2358. [PubMed: 2538507]
26. Kim YT, Lee HJ, Lee SW, et al. Pre-treatment of porcine pulmonary xenograft with desmopressin: a novel strategy to attenuate platelet activation and systemic intravascular coagulation in an ex-vivo model of swine-to-human pulmonary xenotransplantation. Xenotransplantation 2008;15(1):27–35. [PubMed: 18333911]
27. Burdorf L, Azimzadeh AM. Xenogeneic lung transplantation models. Methods Mol Biol 2020;2110:173–196. [PubMed: 32002909]
28. Burdorf L, Riner A, Rybak E, et al. Platelet sequestration and activation during GalTKO.hCD46 pig lung perfusion by human blood is primarily mediated by GPIb, GPIIb/IIIa, and von Willebrand Factor. Xenotransplantation 2016;23(3):222–236. [PubMed: 27188532]
29. Nguyen BN, Azimzadeh AM, Schroeder C, et al. Absence of Gal epitope prolongs survival of swine lungs in an ex vivo model of hyperacute rejection. Xenotransplantation 2011;18(2):94–107. [PubMed: 21496117]
30. Riesbeck K, Dorling A, Kemball-Cook G, et al. Human tissue factor pathway inhibitor fused to CD4 binds both FXa and TF/FVIIa at the cell surface. Thromb Haemost 1997;78(6):1488–1494. [PubMed: 9423800]
31. Dai Y, Vaught T, Boone J, et al. Targeted disruption of the alpha1,3-galactosyltransferase gene in cloned pigs. Nat Biotechnol 2002;20(3):251–255. [PubMed: 11875425]
32. Giraldo A, Ball S, Bondioli K. Production of transgenic and knockout pigs by somatic cell nuclear transfer. Methods Mol Biol 2012;885:105–123. [PubMed: 22565993]
33. Laird CT, Burdorf L, French BM, et al. Transgenic expression of human leukocyte antigen-E attenuates GalKO.hCD46 porcine lung xenograft injury. Xenotransplantation 2017;24(2).
34. Hisashi Y, Yamada K, Kuwaki K, et al. Rejection of cardiac xenografts transplanted from alpha1,3-galactosyltransferase gene-knockout (GalT-KO) pigs to baboons. Am J Transplant 2008;8(12):2516–2526. [PubMed: 19032222]
35. Cooper DK, Ezzelarab M, Hara H, Ayares D. Recent advances in pig-to-human organ and cell transplantation. Expert Opin Biol Ther 2008;8(1):1–4. [PubMed: 18081532]
36. Burdorf L, Stoddard T, Zhang T, et al. Expression of human CD46 modulates inflammation associated with GalTKO lung xenograft injury. Am J Transplant 2014;14(5):1084–1095. [PubMed: 24698431]
37. Westall GP, Levvey BJ, Salvaris E, et al. Sustained function of genetically modified porcine lungs in an ex vivo model of pulmonary xenotransplantation. J Heart Lung Transplant 2013;32(11):1123–1130. [PubMed: 23932853]
38. McGregor CG, Ricci D, Miyagi N, et al. Human CD55 expression blocks hyperacute rejection and restricts complement activation in Gal knockout cardiac xenografts. Transplantation 2012;93(7):686–692. [PubMed: 22391577]
39. Tector AJ, Mosser M, Tector M, Bach JM. The possible role of anti-Neu5Gc as an obstacle in xenotransplantation. Front Immunol 2020;11:622. [PubMed: 32351506]
40. Covarrubias R, Chepurko E, Reynolds A, et al. Role of the CD39/CD73 purinergic pathway in modulating arterial thrombosis in mice. Arterioscler Thromb Vasc Biol 2016;36(9):1809–1820. [PubMed: 27417582]
41. Mohiuddin MM, Singh AK, Corcoran PC, et al. One-year heterotopic cardiac xenograft survival in a pig to baboon model. Am J Transplant 2014;14(2):488–489. [PubMed: 24330419]
42. Harris DG, Benipal PK, Gao Z, et al. Activated Protein C decreases thrombosis on porcine endothelium transgenic for human endothelial protein C receptor-a novel mechanism to decrease porcine xenograft injury. J Surg Res 2014;186(2):579.
43. Yan JJ, Koo TY, Lee HS, et al. Role of human CD200 overexpression in pig-to-human xenogeneic immune response compared with human CD47 overexpression. Transplantation 2018;102(3):406–416. [PubMed: 28968355]

44. Bruel A, Touhami-Carrier M, Thomaidis A, Legrand C. Thrombospondin-1 (TSP-1) and TSP-1-derived heparin-binding peptides induce promyelocytic leukemia cell differentiation and apoptosis. Anticancer Res 2005;25(2A):757–764. [PubMed: 15868907]
45. Mast AE, Stadanlick JE, Lockett JM, Dietzen DJ, Hasty KA, Hall CL. Tissue factor pathway inhibitor binds to platelet thrombospondin-1. J Biol Chem 2000;275(41):31715–31721. [PubMed: 10922378]
46. Jung SH, Hwang JH, Kim SE, Young Kyu K, Park HC, Lee HT. The potentiating effect of hTFPI in the presence of hCD47 reduces the cytotoxicity of human macrophages. Xenotransplantation 2017;24(3).
47. Laird CT, Hassanein W, O'Neill NA, et al. P- and E-selectin receptor antagonism prevents human leukocyte adhesion to activated porcine endothelial monolayers and attenuates porcine endothelial damage. Xenotransplantation 2018;25(2):e12381. [PubMed: 29359469]
48. Kumar A, Villani MP, Patel UK, Keith JC Jr, Schaub RG. Recombinant soluble form of PSGL-1 accelerates thrombolysis and prevents reocclusion in a porcine model. Circulation 1999;99(10):1363–1369. [PubMed: 10077522]
49. Théorêt JF, Bienvenu JG, Kumar A, Merhi Y. P-selectin antagonism with recombinant p-selectin glycoprotein ligand-1 (rPSGL-Ig) inhibits circulating activated platelet binding to neutrophils induced by damaged arterial surfaces. J Pharmacol Exp Ther 2001;298(2):658–664. [PubMed: 11454928]
50. Hayward R, Campbell B, Shin YK, Scalia R, Lefer AM. Recombinant soluble P-selectin glycoprotein ligand-1 protects against myocardial ischemic reperfusion injury in cats. Cardiovasc Res 1999;41(1): 65–76. [PubMed: 10325954]
51. Singbartl K, Ley K. Protection from ischemia-reperfusion induced severe acute renal failure by blocking E-selectin. Crit Care Med 2000;28(7):2507–2514. [PubMed: 10921586]
52. Farmer DG, Anselmo D, Da Shen X, et al. Disruption of P-selectin signaling modulates cell trafficking and results in improved outcomes after mouse warm intestinal ischemia and reperfusion injury. Transplantation 2005;80(6):828–835. [PubMed: 16210972]
53. Tsuchihashi S-I, Fondevila C, Shaw GD, et al. Molecular characterization of rat leukocyte P-selectin glycoprotein ligand-1 and effect of its blockade: protection from ischemia-reperfusion injury in liver transplantation. J Immunol 2006;176(1):616–624. [PubMed: 16365457]
54. Shao HZ, Qin BY. rPSGL-1-Ig, a recombinant PSGL-1-Ig fusion protein, ameliorates LPS-induced acute lung injury in mice by inhibiting neutrophil migration. Cell Mol Biol (Noisy-le-grand) 2015;61(1):1–6.
55. Carraway MS, Welty-Wolf KE, Kantrow SP, et al. Antibody to E- and L-selectin does not prevent lung injury or mortality in septic baboons. Am J Respir Crit Care Med 1998;157(3 Pt 1):938–949. [PubMed: 9517615]
56. Burns JA, Issekutz TB, Yagita H, Issekutz AC. The beta2, alpha4, alpha5 integrins and selectins mediate chemotactic factor and endotoxin-enhanced neutrophil sequestration in the lung. Am J Pathol 2001;158(5):1809–1819. [PubMed: 11337379]
57. Burdorf L, Azimzadeh AM. Progress and challenges in lung xenotransplantation: an update. Curr Opin Organ Transplant 2018;23(6):621–627. [PubMed: 30234737]
58. Gaca JG, Lesher A, Aksoy O, Ruggeri ZM, Parker W, Davis RD. The role of the porcine von Willebrand factor: baboon platelet interactions in pulmonary xenotransplantation. Transplantation 2002;74(11):1596–1603. [PubMed: 12490794]
59. Kanwar S, Woodman RC, Poon MC, et al. Desmopressin induces endothelial P-selectin expression and leukocyte rolling in postcapillary venules. Blood 1995;86(7):2760–2766. [PubMed: 7545469]
60. Connolly MR, Burdorf L, Habibabady Z, et al. Ex vivo perfusion and in vivo xenotransplantation of pig lungs with humanized von willebrand factor demonstrate reduced platelet sequestration. J Heart Lung Transplant 2021;40(4):S146–S147.
61. Cooper DK, Ekser B, Burlak C, et al. Clinical lung xenotransplantation–what donor genetic modifications may be necessary? Xenotransplantation 2012;19(3):144–158. [PubMed: 22702466]
62. Collins BJ, Blum MG, Parker RE, et al. Thromboxane mediates pulmonary hypertension and lung inflammation during hyperacute lung rejection. J Appl Physiol 2001;90(6):2257–2268. [PubMed: 11356791]

63. Pierson RN 3rd, Parker RE. Thromboxane mediates pulmonary vasoconstriction and contributes to cytotoxicity in pig lungs perfused with fresh human blood. Transplant Proc 1996;28(2):625. [PubMed: 8623309]

64. Østerud B, Olsen JO. Pro- and anti-inflammatory effects of histamine on tissue factor and TNFα expression in monocytes of human blood. Thromb Res 2014;133(3):477–480. [PubMed: 24393660]

65. Bhattacharya SK, Das N. Anti-inflammatory effect of intraventricularly administered histamine in rats. Agents Actions 1985;17(2):150–152. [PubMed: 4096304]

66. Burdorf L, Zhang T, Rybak Elena, et al. Combined GPIb and GPIIb/IIIa blockade prevents sequestration of platelets in a pig-to-human lung perfusion model. Xenotransplantation 2011;18:287.

67. Burdorf L, Laird CCT, Harris DG, et al. Pig-to-baboon lung xenotransplantation: extended survival with targeted genetic modifications and pharmacologic treatments. Am J Transplant 2021;22(1):28–45. [PubMed: 34424601]

68. Cimeno A, Barth RN, LaMattina JC. Advances in liver xenotransplantation. Curr Opin Organ Transplant 2018;23(6):615–620. [PubMed: 30300328]

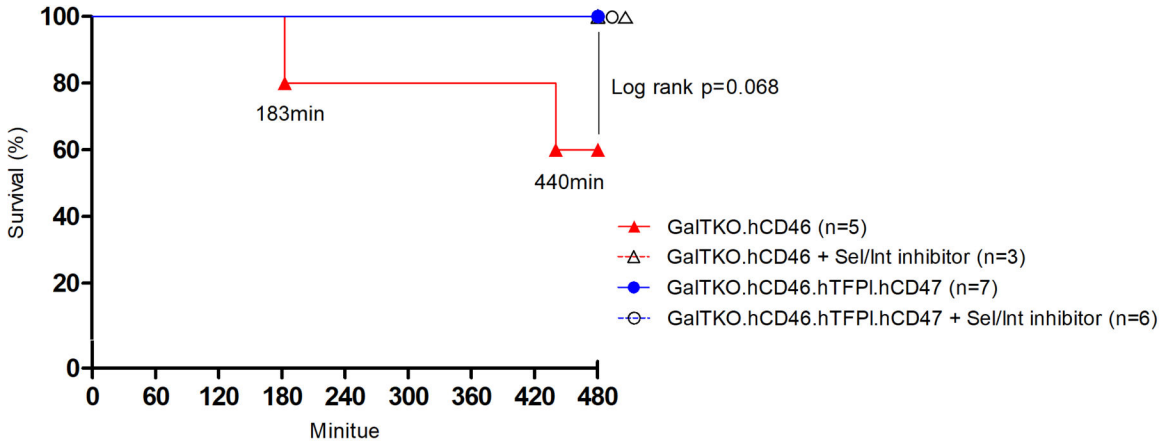

FIGURE 1.

Cumulative lung survival. Survival of *ex vivo* perfused porcine lungs based on predefined lung failure endpoint criteria is illustrated for each experimental group. Two reference lungs failed before 480 min; all GalTKO.hCD46 lungs treated with combined selectin and integrin inhibitor and all hTFPI.hCD47 expressing lungs, with or without combined selectin and integrin inhibition, reached elective termination at 480 min without meeting a lung failure criterion. There was no significant difference in lung survival for hTFPI.hCD47 expressing lungs when compared to GalTKO.hCD46 reference lungs ($p = 0.068$ for the comparison without selectin/integrin inhibition)

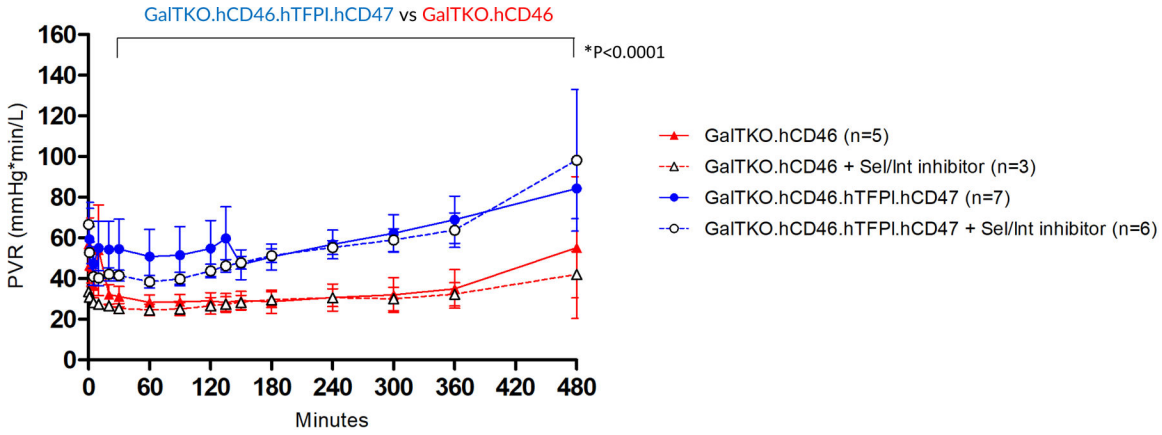

FIGURE 2.

Pulmonary vascular resistance (PVR) during perfusion. PVR is expressed as a function of perfusion time, by experimental group. Time 0 represents measurements obtained during the first minute of lung perfusion. All lungs in both genotypes maintained low-range and very stable PVR values throughout the perfusion. While PVR trended lower with additional selectin and integrin inhibitors in hTFPI.hCD47 lungs during the first 2 h ($P = 0.074$ at 60 min and $P = 0.081$ at 90 min), these differences did not reach the conventional confidence threshold ($P < 0.05$) for assigning statistical significance

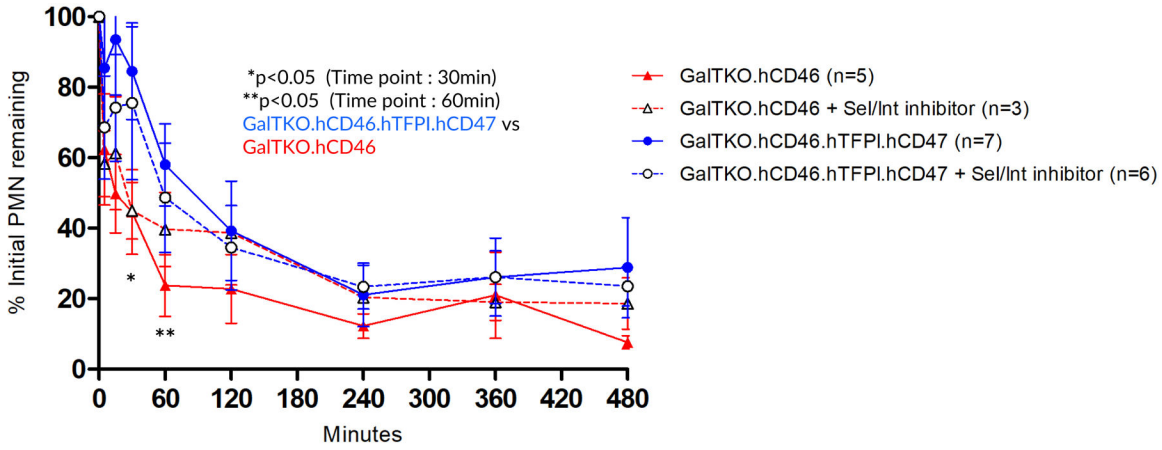

FIGURE 3.

Neutrophil sequestration. Neutrophil counts in pulmonary vein effluent collected serially during *ex vivo* perfusion. Data are expressed as change from the baseline and shown as the mean ± SD of experiments that had not met a lung failure criterion. Neutrophil sequestration was significantly delayed during the first hour in association with hTFPI.hCD47 expression (hTFPI.hCD47 vs. reference at *30 min and **60 min, $p < 0.05$), while additional adhesion pathway inhibition was not associated with further reduction in neutrophil sequestration compared to hTFPI.hCD47 alone

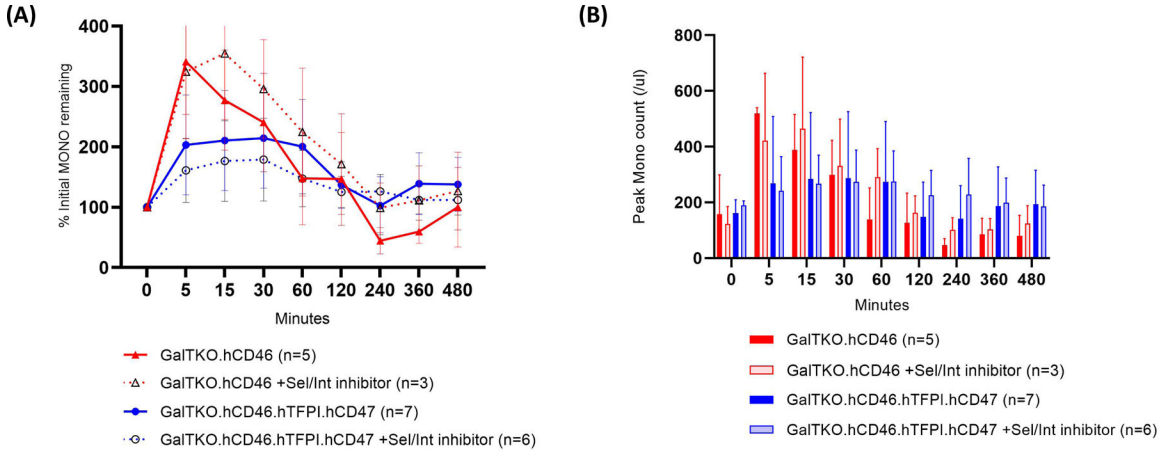

FIGURE 4.

Monocyte elaboration. Monocyte (Mono) elaboration in pulmonary vein effluent during the *ex vivo* perfusion interval. Data are expressed as change from the baseline (A) and expressed as peak absolute Mono count measured after initiation of perfusion (B) and shown as the mean ± SD of experiments that had not met a lung failure criterion. Monocyte counts rose within 5 min after initiation of reference pig lung perfusion with human blood, reflecting release of pig monocytes into the perfusate as confirmed by Sw1-staining (not shown); this phenomenon was consistently seen with or without additional selectin and integrin inhibition. This effect tended to be attenuated in association with hTFPI.hCD47 expression compared to the reference, a trend which did not achieve statistical significance. Subsequent monocyte sequestration was not effectively delayed in association with hTFPI.hCD47 expression, with or without additional adhesion inhibition

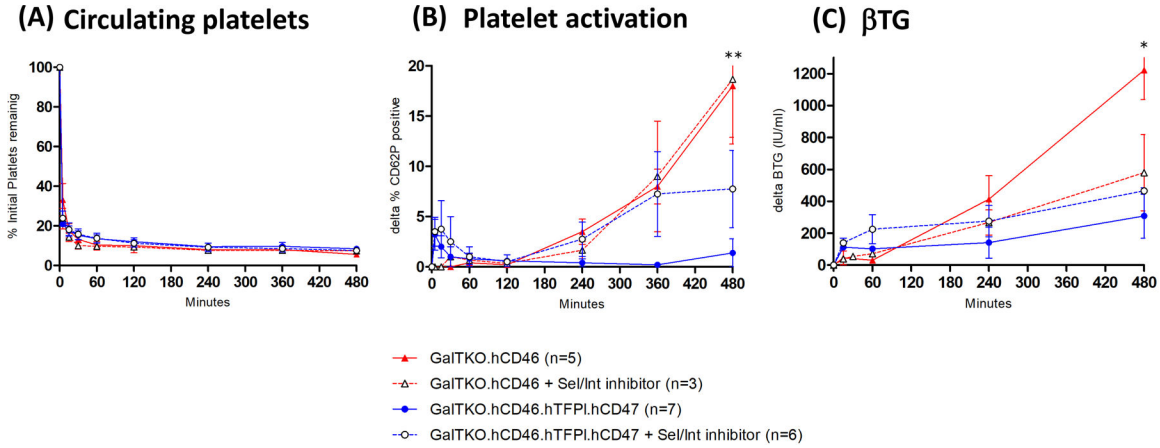

FIGURE 5.

Platelet sequestration and activation. Blood platelet counts measured by flow cytometry in pulmonary vein effluent samples collected serially over the course of *ex vivo* lung perfusion. Platelet sequestration was expressed as the percentage of platelets that remained circulating in the perfusate at each time point (A). Platelet activation was assessed by measuring the proportion of CD41+ platelets expressing CD62P by flow cytometry (B) and by measuring plasma levels of βTG released from platelet granules (C), reflecting cumulative activation of both the sequestered and circulating platelet populations. Data are expressed as change from the baseline and shown as the mean ± SD of experiments that had not met a lung failure criterion

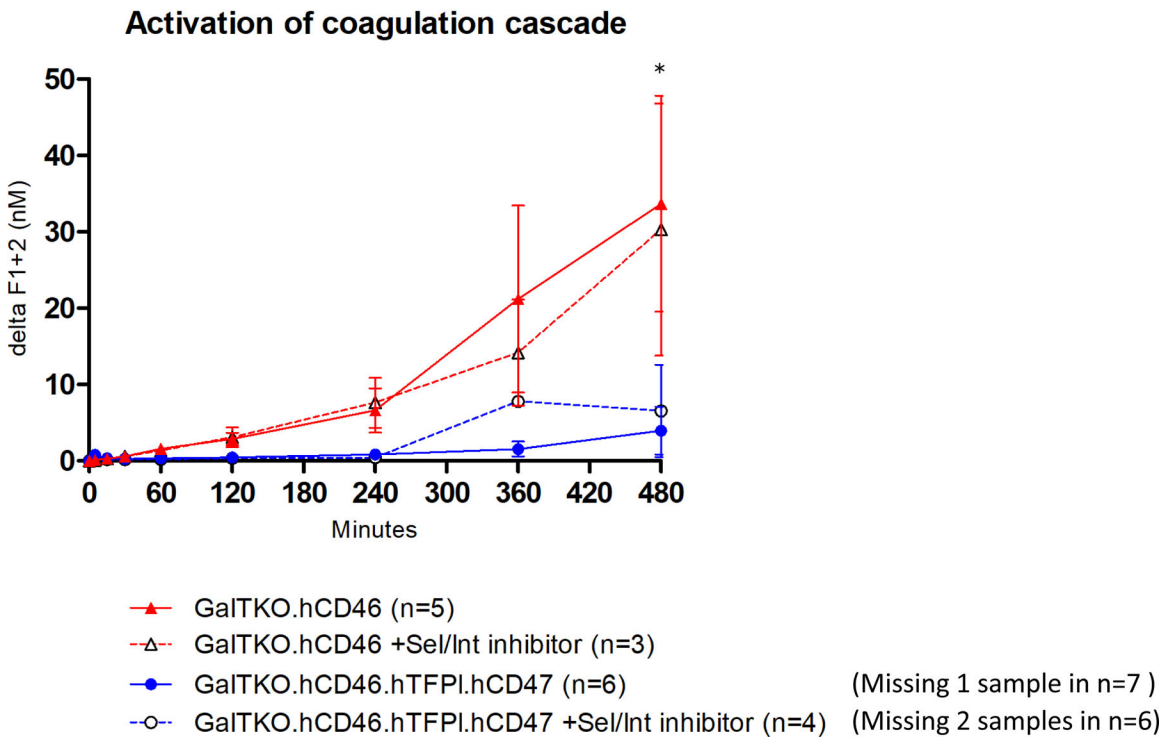

FIGURE 6.

Coagulation cascade activation. Activation of the coagulation cascade was measured by plasma levels of fragments F1+2, reflecting the formation of thrombin from prothrombin. Data are expressed as change from the baseline and shown as the mean ± SD of experiments that had not met a lung failure criterion. Delta F1+2 values showed a similar trend during first 2 h of perfusion in each genotype. hTFPI.hCD47-expressing lungs were associated with significantly decreased coagulation cascade activation at 480 min (4.0±2.0 for hTFPI.hCD47 vs. 33.7±28.3 nmol/L for reference, [$p = 0.0393$]), reflecting a consistent trend also seen at earlier intervals. One hTFPI.hCD47 lung was missing CTAD blood samples and is therefore not included in this analysis

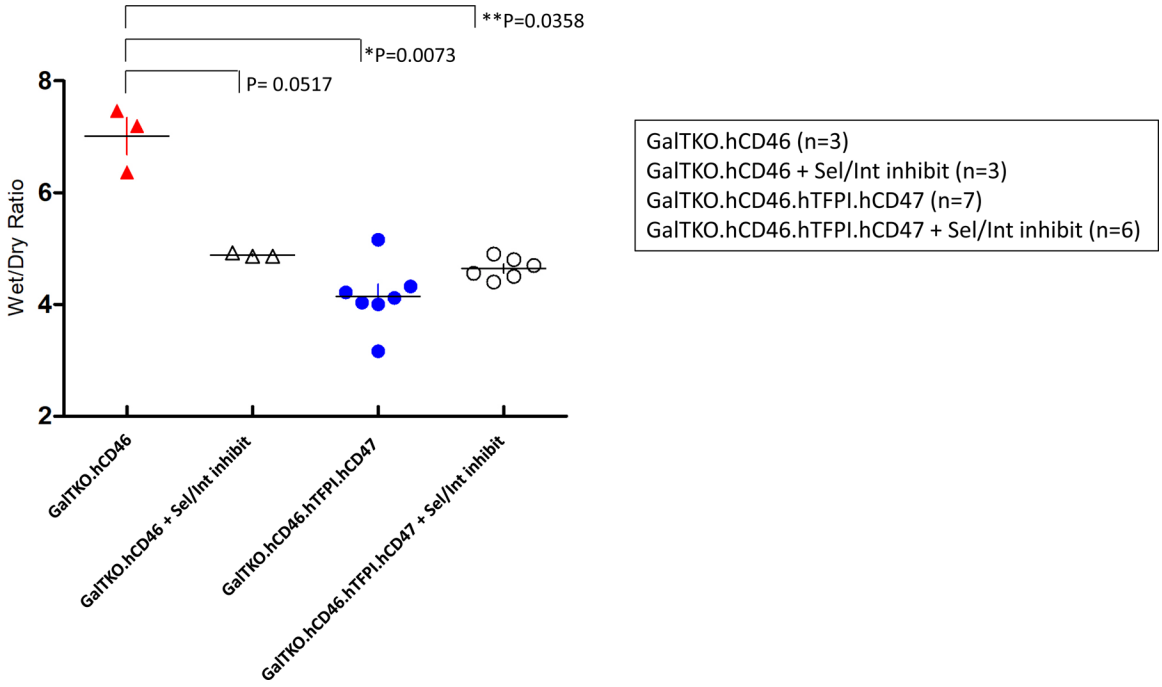

FIGURE 7.

Wet-to-dry weight ratio. Measured as wet-to-dry weight ratio (WDR), pulmonary fluid accumulation after 8 h of perfusion was significantly reduced in hTFPI.hCD47 lungs when compared to GalTKO.hCD46 reference lungs (4.0 ± 1.0 vs. 7.0 ± 1.0, **P* = 0.0073). Additional adhesion inhibitor in hTFPI.hCD47 lungs significantly attenuated the WDR observed in reference lungs (4.8 ± 0.2 vs. 7.0 ± 1.0, ***P* = 0.0358), but did not show further reduction in WDR compared to hTFPI.hCD47 alone. All data are shown as the mean ± SEM of all experiments that were electively terminated at 8 h (two reference lungs that had met a lung failure criterion earlier are excluded)

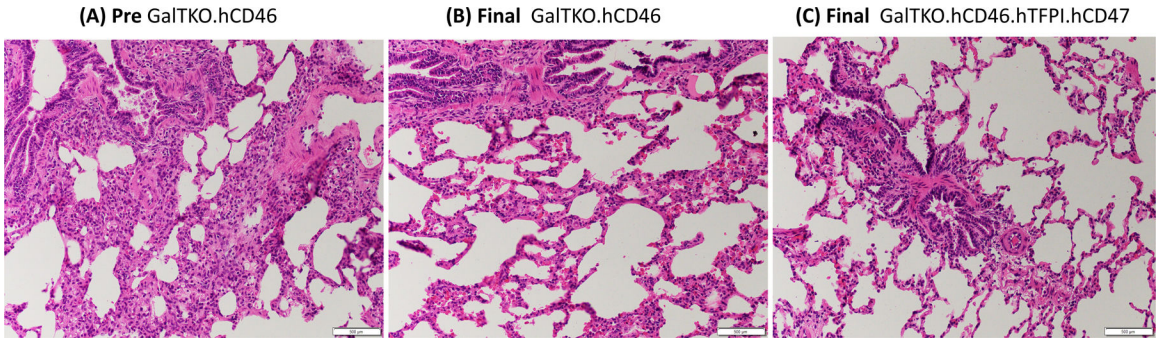

FIGURE 8.

Representative lung histology. Representative pre-perfusion lung histology displayed almost normal microscopic lung anatomy with air-filled alveoli and thin inter-alveolar septae. The final samples from GalTKO.hCD46 reference lung (B) revealed alveolar capillary erythrocyte congestion, interstitial inflammation with neutrophils and other leukocytes adherent to the endothelium of larger vessel, as well as additional bronchial epithelial inflammation. Congestion and inflammation were more severe in reference lungs than in hTFPI.hCD47 lungs (C), which showed relatively well-conserved lung tissue with only mild alveolar capillary congestion and less prominent interstitial, endovascular, and epithelial inflammation. Lung biopsies, H&E, original magnification 20×

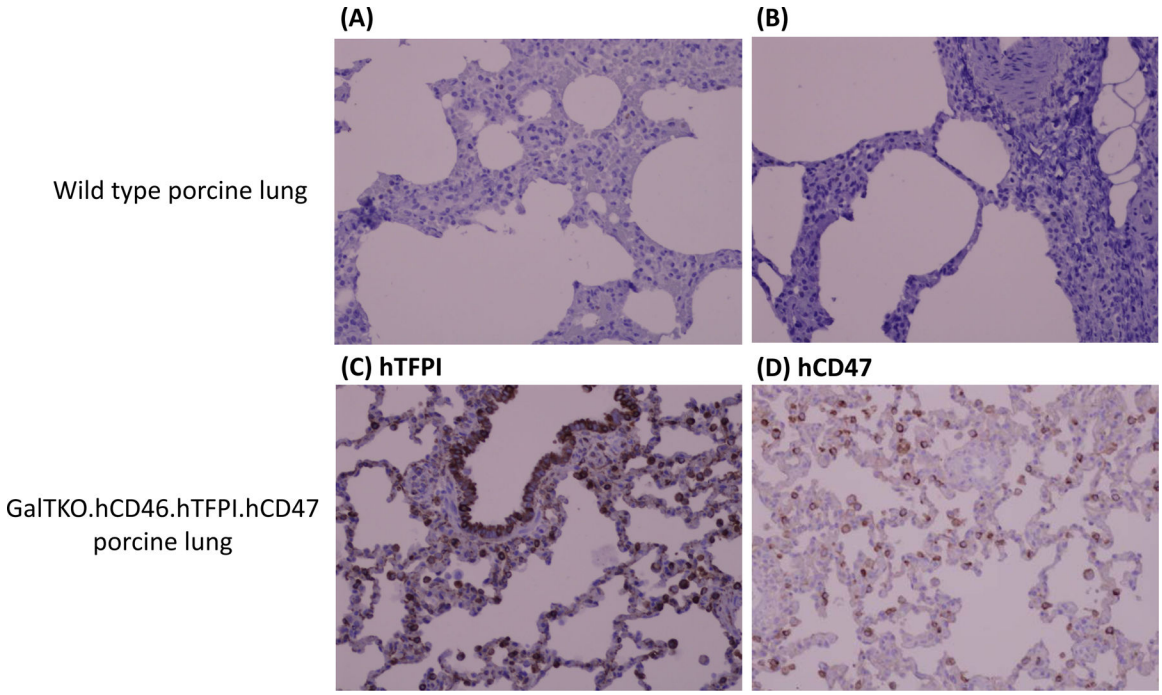

FIGURE 9.

Expression of hTFPI and hCD47 on porcine lung. Expressions of hTFPI (A,C) and hCD47 (B,D) were assessed by immunohistochemistry on formalin-fixed reference (A,B) or hTFPI.hCD47 (C,D) pre-perfusion lung tissues using anti-human TFPI and CD47 antibodies. Positive staining was demonstrated by a deposition of brown pigment at the site of antibody binding. Both hTFPI and hCD47 expression were detected only in hTFPI.hCD47 lungs, with prominent expression in leukocytes for both genes. hTFPI was particularly prominent on alveolar epithelium (C) but was also detected diffusely on vascular endothelium and in alveolar septae in a pattern consistent with prevalent capillary endothelial expression. hCD47 was relatively faintly detected in about 30% of alveolar septae (D), consistent with patchy capillary endothelial expression, and on larger vessel endothelium (not illustrated). Lung biopsies, original magnification 20×